https://doi.org/10.5194/egusphere-2024-851
Preprint. Discussion started: 3 May 2024

Present-day mass loss rates are a precursor for West Antarctic Ice Sheet collapse

Tim van den Akker[1], William H. Lipscomb[2], Gunter R. Leguy[2], Jorjo Bernales[3], Constantijn J. Berends[1], Willem Jan van de Berg[1], Roderik S.W. van de Wal[1,4]

[1]Institute for Marine and Atmospheric Research Utrecht, Utrecht University, Netherlands

[2]Climate and Global Dynamics Laboratory, NSF National Center for Atmospheric Research, Boulder, CO, USA

[3]Danish Meteorological Institute, Copenhagen, Denmark

[4]Department of Physical Geography, Utrecht University, Netherlands

Correspondence to: Tim van den Akker (t.vandenakker@uu.nl)

Abstract. Observations of recent mass loss rates of the West Antarctic Ice Sheet (WAIS) raise concerns about its stability since a collapse would increase global sea levels by several meters. Future projections of these mass loss trends are often estimated using numerical ice sheet models. However, most current models display low skill in reproducing observed mass change rates accurately. Here, we develop a new initialization method that optimizes agreement not only with observations of ice thickness and surface velocity, but also with satellite-based estimates of mass change rates. Starting from this improved present-day state, we generate an ensemble of future projections of Antarctic mass change, covering uncertainties in model choices, parameter values and (observational) input data. Our ensemble displays a slow retreat over several centuries followed by a speed-up that lasts around 200 years. We find that for all ensemble members, the Thwaites and Pine Island glaciers collapse, even though the climate is held constant at present-day values. Our results imply that today's mass loss rates are a precursor of the deglaciation of large parts of the WAIS, which would raise sea levels by at least a meter in the coming centuries, without additional climate forcing.

1 Introduction

The projected Antarctic contribution to global mean sea level (GMSL) rise ranges from 0.03 m (SSP1.9, low end of the likely range) to 0.34 m (SSP8.5, high end of the likely range) in 2100 (Fox-Kemper et al., 2021). This range is reasonably constrained as dynamical processes are not expected to make a large contribution before 2100 (van de Wal et al., 2022). After 2100, however, dynamical processes are highly uncertain, possibly raising GMSL by multiple meters before 2300 (Fox-Kemper et al., 2021, Payne et al., 2021).

https://doi.org/10.5194/egusphere-2024-851
Preprint. Discussion started: 3 May 2024

One uncertain process is the Marine Ice Sheet Instability (MISI; Pattyn et al. (2018)), which could drive the unforced irreversible retreat of marine-terminating glaciers. MISI might occur for parts of the ice sheet where unbuttressed outlet glaciers terminate on a retrograde-sloping, submerged bedrock, due to a positive feedback between the flux across the grounding line (GL, the transition line between a grounded ice sheet and a floating ice shelf) and the ice thickness at the GL. Thwaites Glacier (TG) and Pine Island Glacier (PIG), in the Amundsen Sea region of the West Antarctic Ice Sheet (WAIS), are in such locations and may be vulnerable to MISI. It is suggested that those glaciers are already undergoing MISI-like retreat (Favier et al., 2014, Joughin et al., 2014).

Currently, the Thwaites GL retreats by up to 1.2 km per year on the eastern shelf and up to 0.9 km per year along the western margin (Milillo et al., 2019), and the GL of PIG retreated 31 km in 20 years (Rignot et al., 2014). Warm Circumpolar Deep Water (CDW) and related higher basal melt rates have been observed under Pine Island Glacier (Jacobs et al., 2011) since the early 1990s, and results from a model study show that CDW intrusions have coincided with PIG speedup (Thoma et al., 2008, Jenkins et al., 2016). As a result, the Amundsen Sea Embayment (ASE, which contains TG and PIG) is currently the largest contributor to Antarctic Ice Sheet (AIS) mass loss (Rignot et al., 2019, Smith et al., 2020). Further retreat of PIG and TG would increase ice drainage from these basins into the ocean, eventually triggering the collapse (i.e. relatively fast, potentially irreversible ungrounding and ice loss) of a significant part of the WAIS over several centuries (Sun et al., 2020).

Several modelling studies have assessed the potential for ASE collapse under current climate forcing. One study (Joughin et al., 2014) argued that under present-day melt rates, TG might already be on a trajectory toward irreversible retreat; moderate retreat in this century will likely be followed by a phase of rapid collapse beginning in the next 200 to 900 years. Another study (Favier et al., 2014) used three ice sheet models to show that PIG is now undergoing an unstable 40-km retreat (but makes no projections after this). The retreat could be reversed by sufficient ocean cooling (Favier et al., 2014). Both studies mention MISI as the main driver of retreat. Subsequently, several studies suggest that TG and PIG are unstable under the current climate and could collapse on a timescale of a few centuries (Joughin et al., 2014, Arthern and Williams, 2017, Golledge et al., 2021, Coulon et al., 2023). In contrast, other studies have argued that under the present-day climate, TG and PIG are relatively stable (Feldmann and Levermann, 2015, Arthern and Williams, 2017, Garbe et al., 2020, Rosier et al., 2021, Reese et al., 2023). For example, one study (Reese et al., 2023) ran an ensemble of model simulations in which TG and PIG collapse only on millennial timescales, with a GMSL contribution never exceeding 1 mm/yr. Some models projected accelerated retreat leading to a collapse only when ocean thermal forcing increases by 1–2 K relative to a preindustrial or 20th century equilibrium (Garbe et al., 2020, Lipscomb et al., 2021). There are few historical observations of Southern Ocean temperatures, so it is unknown how much the ASE has warmed in the past century, and if the warming needed to drive such a retreat has already happened. It is therefore not possible to conclude from those studies whether the glacier retreat in the WAIS will sustain and eventually accelerate under present day climate conditions.

https://doi.org/10.5194/egusphere-2024-851
Preprint. Discussion started: 3 May 2024

Studying ASE stability under current climate conditions requires century-scale model simulations. For such long-term projections, uncertainties arise from four main sources (Aschwanden et al., 2021): suboptimal ice sheet model initialization, incomplete physical understanding of important processes, numerical model uncertainty, and uncertainty in the climate forcing. With respect to initialization, ice sheet models struggle to represent observed present-day mass change rates (Seroussi et al., 2019). Representing these decadal-long present-day mass change rates right is essential for reliable projections, as these changes are the primary observable of the dynamic state of the ice sheet.

Broadly, two methods are used to initialize ice sheet models: data assimilation and spin-up. In the first, data assimilation (DA) methods (Gudmundsson et al., 2012, Larour et al., 2012, Cornford et al., 2015, Hoffman et al., 2018, Bradley and Arthern, 2021) are used to iterate toward a specific state. For example, based on the observed ice thickness, the ice surface velocities are calculated and compared to observations. Uncertain parameters are tuned iteratively until the velocities converge to a state close to observations. This has the advantage that the resulting ice sheet matches the observed thickness and velocities at the start of a forward run, without being necessarily in steady state. However, the model drift, when run forward, can be erratic if ice thickness and surface velocity observations are not mutually consistent. Subsequently, where physically realistic, the drift still does not necessarily equal the observed mass change rates, as, so far, matching the observed mass change is not used as optimalisation target.

The other approach is the spin-up method (Winkelmann et al., 2011, Pollard and DeConto, 2012, Greve and Blatter, 2016, Quiquet et al., 2018, Lipscomb et al., 2019, Berends et al., 2021, Berends et al., 2022) consists of a run with paleoclimatic or preindustrial forcing during which the ice sheet can freely evolve. Uncertain parameter values can be tuned, to nudge variables like ice thickness and surface velocities toward present-day observed values. The resulting ice sheet is ideally close to observations and in near equilibrium with little drift. The modeled ice sheet can also be tuned to historical (e.g., 20th century) estimates or observations, and then advanced to the present-day using GCM forcing, to avoid an unrealistic steady state at the start of a forward run (Coulon et al., 2023, Reese et al., 2023). A further challenge in modeling the observed present-day mass change rates through the ice-sheet model initialization is that the magnitudes and spatial patterns of historical sub-shelf melt rates are poorly constrained by observations and models. Global climate models (GCMs) generally do not simulate large Amundsen Sea warming in the recent past (Naughten et al., 2022). Thus, forcing an ice sheet model with ocean output from GCMs will tend to underestimate current melt and thinning.

We therefore developed an addition to the spin-up method. Our initialization procedure expands this method by equilibrating the modeled ice sheet to the mass balance corrected with the observed mass change rates at individual grid points, before starting future runs. The observed mass change rates are derived from satellite-observed surface elevation change rates (Smith et al., 2020), corrected for firn processes and glacial isostasy. This procedure avoids the potential DA biases, reduces the uncertainty associated with direct GCM forcing, and circumvents the need to represent the AIS in its unknown pre-

https://doi.org/10.5194/egusphere-2024-851
Preprint. Discussion started: 3 May 2024

industrial state. We apply this method to the Community Ice Sheet Model (CISM, Lipscomb et al. (2019), Lipscomb et al. (2021)) at 4 km horizontal resolution, and the Utrecht Finite volume ice sheet model UFEMISM (Berends et al., 2021). These ice sheet models, the initialization method, and the subsequent forward runs are described in detail in Section 2. In Section 3, we demonstrate that the new initialization procedure results in a modeled present-day state by CISM which is in very good agreement with observations (ice thickness RMSE 34 m, ice surface velocity RMSE = 121.2 m/yr, GL position on average 1.5 km from the observed GL), and importantly has the same disequilibrium as observed. In Section 4 we discuss the default forward run, starting from this state, under sustained present-day atmosphere and (inverted) ocean forcing, purposely excluding further climate forcing. Furthermore, we test an extensive variety of physical approximations and parameter settings in CISM and repeat the default simulation with UFEMISM to show that the observed retreat of TG and PIG is robust and will eventually accelerate even under current climate conditions (Section 5). This manuscript ends with conclusions in Section 6.

2 Methods

2.1 CISM

The Community Ice Sheet Model (CISM; (Lipscomb et al., 2019, Lipscomb et al., 2021)) is a thermo-mechanical higher-order ice sheet model, which is part of the Community Earth System Model version 2 (CESM2, Danabasoglu et al. (2020)). This study primarily uses CISM v2.1 and builds on earlier applications of CISM to Antarctic Ice Sheet retreat (Lipscomb et al., 2021, Berdahl et al., 2023). CISM is run at 4 km resolution with a vertically integrated higher-order approximation to the momentum balance (Goldberg, 2011, Robinson et al., 2022), with a regularized Coulomb sliding law (Zoet and Iverson, 2020) as basal boundary condition. We apply the present-day surface mass balance from RACMO version 2.3p2 (Van Wessem et al., 2018). Basal melt rates are calculated using a quadratic relation with a thermal forcing observational dataset (Jourdain et al., 2020). UFEMISM v1.0 (Berends et al., 2021) is used to test whether the results depend on the numerical features of a single model. Variable names and parameter values used in the following text are summarized in Tables 1 and 2.

Table 1. Variables used in this study.

Variables	Definition
b	Bedrock height above sea level
$bmlt$	Basal melt rates under floating ice
C_c	Basal friction coefficient (Coulomb C)
C_r	Basal friction relaxation target
H	Modeled ice thickness

https://doi.org/10.5194/egusphere-2024-851
Preprint. Discussion started: 3 May 2024

H_f	Ice thickness above floatation
H_{obs}	Observed ice thickness
N	Effective pressure
TF_{base}	Thermal forcing from Jourdain et al. (2020) applied at the ice shelf draft
u_b	Basal velocities magnitude
δT	Ocean temperature correction
τ_b	Basal shear stress

115

Table 2. Parameters and their units and values used in this study.

Parameters	**Values**	**Units**	**Defintion**
c_{pw}	3974	J kg^{-1} K^{-1}	Specific heat of seawater
g	9.81	m s^{-2}	Gravitational acceleration
H_0	100	m	Ice thickness scale in the inversion
L_f	3.34 * 10^5	J kg^{-1}	Latent heat of fusion
m	3	-	Basal friction exponent
T_r	0	K	Relaxation target of the ocean temperature inversion
u_0	200	m yr^{-1}	Yield velocity
p	0.5	-	Exponent in effective pressure relation
r	0.5	-	Strength of inversion relaxation
ρ_i	917	kg m^{-3}	Density of ice
ρ_w	1027	kg m^{-3}	Density of ocean water
τ	100	yr	Time scale in the inversion
γ_0	30000	m yr^{-1}	Basal melt rate coefficient

2.1.1 Basal friction

120 In the default configuration, basal friction is parameterized using a basal sliding law based on laboratory experiments (Zoet and Iverson, 2020). This sliding law combines elements of ice sliding on a hard bed (e.g., bedrock) with sliding on deformable soft beds (e.g., saturated till). Its end cases are Weertman-style sliding, with basal velocities dependent on some power of the basal friction, and Coulomb sliding, with basal friction and velocities decoupled. The former mechanism

https://doi.org/10.5194/egusphere-2024-851
Preprint. Discussion started: 3 May 2024

usually dominates where the ice sheet is frozen to the bed, while the latter describes fast-flowing outlet glaciers such as Pine Island and Thwaites Glaciers. In CISM, the basal sliding law is implemented as follows:

$$\tau_b = C_c N \left(\frac{u_b}{u_b + u_0}\right)^{\frac{1}{m}} \quad (1.1)$$

where C_c is a unitless parameter controlling the strength of the Coulomb sliding, In CISM, C_c corresponds to $tan\,\phi$ of Zoet and Iverson (2020), in which ϕ is the friction angle, a material property of the subglacial till. Since C_c is poorly constrained by theory and observations, we use it as a spatially variable tuning parameter, which we tune in the following way using a nudging method (Lipscomb et al., 2021):

$$\frac{dC_c}{dt} = -C_c \left[\left(\frac{H - H_{obs}}{H_0 \tau}\right) + \frac{2}{H_0}\frac{dH}{dt} - \frac{r}{\tau} ln \frac{C_c}{C_r}\right] \quad (1.2)$$

in which H is the modeled ice thickness, H_{obs} the observed ice thickness, and C_r the relaxation target for C_c. H_0, τ and r are empirical constants used to vary the size of each term. The relaxation target is a 2D field that inhibits very high and low values of C_c. It is based on elevation, with lower values at low elevation where soft marine sediments are likely more prevalent. We chose targets of 0.1 for bedrock below -700 m asl and 0.4 for 700 m asl, with linearly interpolation in between. Our values for H_0 and τ are respectively 100 m and 100 yr.

The effective pressure N is the pressure at the ice–bed interface, equal to the difference between the ice overburden pressure and the subglacial water pressure. The effective pressure is lowered near GLs to represent the connection of the subglacial hydrological system to the ocean (Leguy et al., 2014):

$$N = \rho_i g H \left(1 - \frac{H_f}{H}\right)^p \quad (1.3)$$

where ρ_i is the density of ice, g is gravitational acceleration, H is the ice thickness, and p is an exponent between 0 and 1 (with a larger value implying a stronger ocean connection). The flotation thickness H_f is the height of an ice column resting on bedrock below sea level ($b < 0$) at hydrostatic equilibrium; it is given by

$$H_f = \max\left(0, -\frac{\rho_w}{\rho_i} b\right) \quad (1.4)$$

where ρ_w is the density of sea water and b is the bedrock elevation. Runs in this study were done with $p = 0.5$ unless stated otherwise.

2.1.2 Basal melt rates

Beneath grounded ice, CISM computes basal melt rates based on the net of geothermal, frictional, and conductive heat fluxes

https://doi.org/10.5194/egusphere-2024-851
Preprint. Discussion started: 3 May 2024

at the bed. In our runs, however, there is no coupling between basal water and sliding parameters. Beneath floating ice, we use the ISMIP6 local parameterization (Jourdain et al., 2020):

$$bmlt = \gamma_0 \left(\frac{\rho_w c_{pw}}{\rho_i L_f}\right)^2 (\max[TF_{\text{base}} + \delta T, 0])^2 \quad (1.5)$$

The max function ensures non-negative melt rates; negative rates imply refreezing (accretion), which is not represented. We tune δT to optimize the ice thickness agreement with observations, like Eq. (1.2):

$$\frac{d(\delta T)}{dt} = -\delta T \left[\left(\frac{H - H_{obs}}{H_0 \tau}\right) + \frac{2}{H_0}\frac{dH}{dt}\right] + \frac{(T_r - \delta T)}{\tau} \quad (1.6)$$

where T_r is a relaxation target for the temperature correction. Ideally, the correction is small, and therefore we set $T_r = 0$ everywhere. Melt rates are sensitive to γ_0. We chose a default value $\gamma_0 = 3.0 \times 10^4$ m/yr, for which the average δT in the Thwaites basin at the end of the transient spin-up is close to 0. In other words, we assumed that the observed ocean temperatures in this region are of the right magnitude to drive basal melt rates consistent with observations.

2.1.3 Grounding line subgrid-scale parameterization

The GL is not explicitly modeled in CISM but follows from the hydrostatic balance. Thus, the modeled GL cuts through cells, with some cells partly grounded and partly floating. To prevent abrupt jumps in modeled quantities at the GL, we use a GL parameterization (Leguy et al., 2021). We define a flotation function,

$$f_{\text{float}} = -b - \frac{\rho_i}{\rho_w} H \quad (1.7)$$

which varies smoothly from negative for grounded ice to positive for floating ice. (For floating ice, f_{float} is the thickness of the ocean cavity). f_{float} is used to compute the floating fraction as a percentage of grid cell area by interpolating its value from cell vertices to the cell areas scaled to the cavity thickness. The grounded and floating fraction of a cell are then used to scale basal friction and basal melting.

2.1.4 Calving

There are several calving laws in the literature, including applications to Antarctic ice shelves (e.g. (Yu et al., 2019), Greene et al. (2022), Wilner et al. (2023)). However, there is no agreed-upon best approach to Antarctic calving, and most calving laws struggle to reproduce the observed calving front at multiple locations simultaneously (Amaral et al., 2020). Since we are unable to attain an accurate initial state with a physically-based calving law, we err on the conservative side by applying a no-advance calving scheme. With this scheme, the calving front cannot advance beyond the observed present-day calving front. It can retreat, but only when it thins below a threshold thickness of 1 m. In most places, the calving front does not move. This

https://doi.org/10.5194/egusphere-2024-851
Preprint. Discussion started: 3 May 2024

is a conservative approach; in practice, we would expect the calving front to move inland and therefore provide less buttressing than the model suggests.

2.2 UFEMISM

We repeated the main experiment with the Utrecht FinitE VoluMe Ice Sheet Model (UFEMISM) (Berends et al., 2021). We use the same initialization procedure, discussed in more detail later, and climate forcing as in the default CISM setup but apply a different momentum balance approximation and discretization scheme.

UFEMISM is a thermo-mechanical ice-sheet model designed for long-term simulations at targeted high resolution (Berends et al., 2021). UFEMISM discretizes the hybrid SIA/SSA approximation to the stress balance (Bueler and Brown, 2009) and other physical equations on a dynamic adaptive triangular mesh. In this study, mesh resolution ranges from ~4 km at the grounding lines of PIG and TG, to ~60 km over slow-moving inland ice. Here we apply a Budd-type sliding law, see Eq 1.8 (sometimes referred to as a regularized Coulomb sliding law (Joughin et al., 2019)), which contains spatially-varying friction coefficients that aim to represent subglacial substrate conditions.

$$\tau_b = C_p u_b^{\frac{1}{m}} N^q \tag{1.8}$$

We invert for C_p by nudging toward a target geometry (Pollard and DeConto, 2012, Bernales et al., 2017). As part of this nudging method, UFEMISM simultaneously inverts for sub-shelf melt rates and the corresponding ocean temperatures needed to reproduce the target geometry over ice-shelf sectors (Bernales et al., 2017). Both calibrations are performed during model initialization, which brings the modeled ice sheet to a state of equilibrium with a prescribed set of boundary conditions. For this study, friction coefficients and ocean temperatures are inverted during the first 90,000 model years of the initialization, after which their values are kept fixed in time. The model is then run for another 10,000 years, which allows it to evolve unperturbed until equilibrium is attained.

2.3 Initialization methods

We apply two initialization methods. The first method, the equilibrium initialization strategy, nudges basal friction parameters and ocean temperatures to optimize the agreement of ice thickness with observations, allowing a modest error (an error scale of H_0 = 100 m in Eqs. (1.2) and (1.6)) to avoid overfitting, but without considering the observed mass change rates. This results in a steady state, where the integrated SMB is in equilibrium with the modeled calving and basal melt fluxes. This typically takes 10^4 model years.

The second initialization procedure, referred to as the transient spin-up, allows both ice-flow models to reach a geometry in agreement with observations like the result of the equilibrium initialization, while also allowing the ice to thin or thicken in agreement with satellite observations at the start of the forward run (i.e., at the present day). We start with the above-described

https://doi.org/10.5194/egusphere-2024-851
Preprint. Discussion started: 3 May 2024

procedure to achieve an ice-sheet configuration by nudging the ice thickness toward observations and while simultaneously calibrating basal friction coefficients under grounded ice and ocean temperatures below ice shelves. Our goal is to create the observed dynamic disequilibrium, so we want to include the observed mass change rates as a target. However, because the nudging procedure (by necessity) occurs over model time, the ice geometry will shift away from observations once the mass change rates are applied. We temporarily prevent that from happening by re-supplying the lost ice in areas that are thinning and removing the accumulated ice in areas that are thickening. If we set this "correction term" equal to minus the observed mass change rates, then by the time the nudging procedure has achieved a constant geometry, we will have trained the model to produce ice fluxes that are (nearly) identical to reality.

In our transient initialization method, we therefore "train" the ice sheet model to equilibrate toward a state in which observed mass change rates are implicitly accounted for. For ice shelves with rapid thinning observed, the mass correction is positive, which allows ocean temperatures to remain warmer than without the correction. Similarly, where grounded ice is thinning, we apply a positive mass correction that allows basal friction to be weaker than it would be otherwise.

The default experiment taking off from the transient initialization is compared against an extensive set of parameter and model choice experiments, to assess the effect of uncertain or crudely represented physical processes and parameter values. We designed the set of experiments conservatively; we mostly selected model choices that would make the ice sheet theoretically more stable. See Fig. 4, Table 3, and the Extended Data for a detailed description.

2.8 Forward simulations

A forward simulation departing from the transient initialization method starts by stopping the inversion and simultaneously removing the correction term from the mass balance. As a result, the ice will start to thin/thicken at (almost) exactly the observed rates, with ideally only a very small model drift. These simulations are continued without additional climate forcing, to assess the impact of the present-day mass changes rates on the (unforced) evolution of the AIS, and thereby the sea-level contribution over time. The unforced future simulation using this initialization strategy is referred to from now on as the "default experiment". We stress that the future evolution does not include future climate forcing, so the modeled future evolution of the ice sheet is purely the result of the response to the present-day imbalance. Complementary to these default experiments, we verified if model drift is negligible with forward runs in which the mass balance correction term remains included. These results show that the model drift is negligible (Fig. S6). On longer timescales (2 kyrs), the model tends to grow to a slightly advanced state for PIG and the Dotson ice shelf. These advances are mostly due to local positive feedback between the ice shelf geometry and basal melt rates, as these advances are largely reduced in a forward run with time-constant basal melt rates (not shown).

https://doi.org/10.5194/egusphere-2024-851
Preprint. Discussion started: 3 May 2024

In forward simulations, the ice sheet starts to retreat after the mass correction term in the spin-up is removed. This has implications for the inverted C_c and ocean temperatures in cells that change from grounded to floating or vice versa. If grid points initialized as grounded ice become afloat, we extrapolate the average ocean temperature corrections under the shelf from the end of the initialization. If initially floating grid points become grounded, we use an elevation-dependent parameterization to estimate the local C_c.

2.5 Missing processes

We note two missing processes that could affect the ice evolution. First, the mass change rates on grounded ice are controlled by parameters in the basal sliding law. After the initialization phase, C_c is kept constant during forward runs, not accounting for future evolution of the ice–bed interface (e.g., increased basal meltwater that could enhance sliding (Dow, 2019, Kazmierczak et al., 2024)). Possible feedbacks (see for example van der Wel et al. (2013) , Rémy and Legresy (2004)) between the ice flow and the bed are only partly represented through the basal friction law and the calculation of the effective pressure on bedrock below sea level (which roughly represents a hydrological connection to the ocean).

Second, as ice shelves melt and retreat, adding freshwater to the ocean, there is no feedback on ocean temperature or salinity. There are several ways for the freshwater flux from a collapsing WAIS to influence the ocean properties of the Amundsen Sea and the Southern Ocean. For example, cooling of the Southern Ocean sea surface, warming of the deeper ocean layers, and reduced Antarctic Bottom Water formation (Swart et al., 2023). The freshwater input can directly influence the basal melt rates by stratifying the ocean just beyond the shelves, thus trapping heat in the subsurface ocean and ultimately increasing the heat transport into the cavities, resulting in higher basal melt rates (Flexas et al., 2022). An earlier study found a relation between freshwater flux and sea ice formation and the presence of warm and dense water in large AIS cavities: a freshwater flux stabilizes and stratifies the ocean flow in cavities, and prevents further warm water from flowing in (Hellmer, 2004). This is a negative feedback, in contrast to the study by Flexas et al. (2022). The exact effect of a large freshwater pulse into the ocean surrounding the AIS is unknown (Swart et al., 2023). Since we use a standalone-ice sheet model in this study, and no consensus has been reached on the effect of the freshwater flux, we did not parameterize this effect. In future studies, freshwater feedbacks could be added by coupling the ice sheet model to a cavity-resolving ocean model.

https://doi.org/10.5194/egusphere-2024-851
Preprint. Discussion started: 3 May 2024

3. Results: Transient present-day state

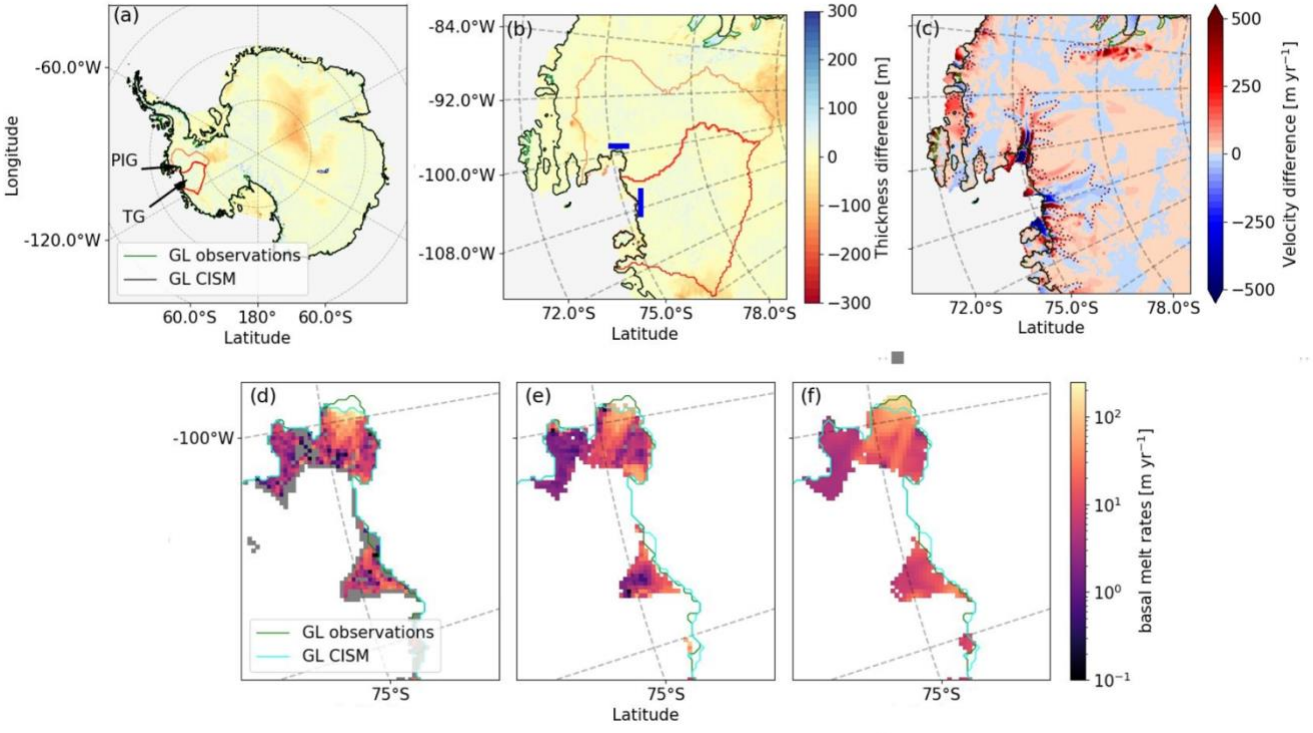

Figure 1. Initialized state of the Antarctic Ice Sheet. (Top row) Ice thickness difference between the final state of the transient initialization and observations for entire Antarctica (RMSE = 34 m, (a)) and the ASE region (RMSE = 19.3 m, (b)). Black contours represent the modeled GL. The observed GL (green) is visible only where the modeled and observed GL deviate in position, for example at the PIG GL. Red and orange contours are drawn around the TG and PIG basins, respectively. Blue bars indicate the locations of the cross sections where the fluxes are calculated in Fig S1. (c) Surface ice velocity difference with respect to observations of Rignot et al. (2019). Positive differences indicate locations where CISM overestimates velocities. Observed surface velocities of 100 (outer) and 500 (inner) m/yr are contoured by black dots, to highlight fast-flowing regions with large velocities and gradients. For the ASE, the velocity RMSE = 99 m/yr. For ASE shelves only, the velocity RMSE = 216 m/yr. (Bottom row panel d,e,f) Basal melt rates (zero basal melt is marked by grey cells, white cells contain no data) of CISM ((d), integrated flux of 106 Gt/yr), Adusumilli et al. (2020) ((e), integrated flux of 94 Gt/yr) and Rignot et al. (2013) ((f), integrated flux of 149 Gt/yr).

Figure 1 shows the modeled CISM state at the end of the transient initialization. The resulting initialized state in UFEMISM is shown in Fig. S2, and the result of the CISM equilibrium initialization in Fig. S3. The thickness bias over the WAIS is low, and the GL closely follows observations, with an average 1.5 km difference (calculated as the average distance between the

https://doi.org/10.5194/egusphere-2024-851
Preprint. Discussion started: 3 May 2024

modeled GL position and the closest observed GL position). The modeled GL for PIG is shifted seaward by 5–10 km. The modeled basal melt rates and melt patterns beneath floating ice agree well with the values from Rignot et al. (2013) and Adusumilli et al. (2020), with an integrated melt flux within the range of the two datasets.

The modeled ice surface velocities are in good agreement with observations, even though they are not a target for assimilation. The root mean square error (RMSE) of the ice surface velocities is comparable to other ISMIP6 models (Seroussi et al., 2020), of which the range is 100 – 400 m/yr, where many are optimized to match observed velocities. Modeled PIG and Thwaites velocities are too low midstream and too high in the lateral margins, possibly because of the lack of brittle processes in CISM. These regions are heavily crevassed (Lhermitte et al., 2020); taking crevasses into account would weaken the ice and speed up the main flowlines and slow down the margins. Since these are compensating errors, the integrated ice fluxes across the GLs of TG and PIG are close to the observations of Morlighem et al. (2020) (Fig. S1). As the ice flux is more important for the existence of the shelf than grid-cell-based velocities, we believe that the model's dynamic characteristics (very accurate GL, good flux across the GL, and ice thickness changes almost equal to observations) are sufficient for our continuation experiments.

In the equilibrium initialization, ocean temperatures in the Amundsen Basin on average must be reduced by ~1 K compared to the thermal forcing dataset from Jourdain et al. (2020) to reproduce the observed ice shelf geometry. This is likely caused by an underestimation of modelled ice velocities in this region during the equilibrium initialization (Fig S3). As a result, the grounding line flux is lower (see Fig. S1), therefore, lower basal melt rates and in general colder ocean conditions are required to model the observed ice shelf geometry, compared to observations. Much smaller corrections of either sign are needed within the transient initialization method. This brings the basin average tuned ocean temperature perturbations closer to zero, highlighting that only a small correction on the ocean dataset is sufficient to produce the initialized state in equilibrium with the observed mass change rates using the ISMIP6 basal melt rate formulation, Eq. (1.5). Ignoring the observed mass changes rates in the initialization procedure results in a larger ocean temperature correction term.

The observed and modeled ice thickness change rates in the first years after the start of a continuation run are shown in Fig. S4. The modeled mass change rate pattern over the first 5 years has broadly the same characteristics as the observations. The thinning rate of PIG decreases while the thinning rate of TG increases, which is likely the result of grounding line movement and buttressing. In fact, a pulse-like pattern is visible in the modeled mass change rates pattern in the first 50 years of a continuation run, where thickening or thinning rates originate from grounding line changes and are subsequently advected in the direction of the calving front (see Supplementary Movie 1).

https://doi.org/10.5194/egusphere-2024-851
Preprint. Discussion started: 3 May 2024

4. Results: Future state

In the default continuation experiment without further climate forcing, AIS mass loss is dominated by the collapse of TG (including the neighboring Smith, Pope, and Kohler glaciers) and PIG (Fig. 2). In the first four centuries, mass loss is comparable to the current observed rates. During this period, the total AIS mass loss averages 0.5 mm GMSL yr^{-1}, slightly less than the combined effect of PIG and TG, because there is currently some EAIS thickening, primarily in Dronning Maud Land (Smith et al., 2020), which persists in the continuation experiment (Fig. 2a). We can furthermore identify a shallow ridge in the TG bedrock profile approximately 45 km upstream of the present-day GL, which acts as the last pinning point before the accelerated collapse begins (see line *AB* in Fig. 2a and Extended Data Fig. S7).

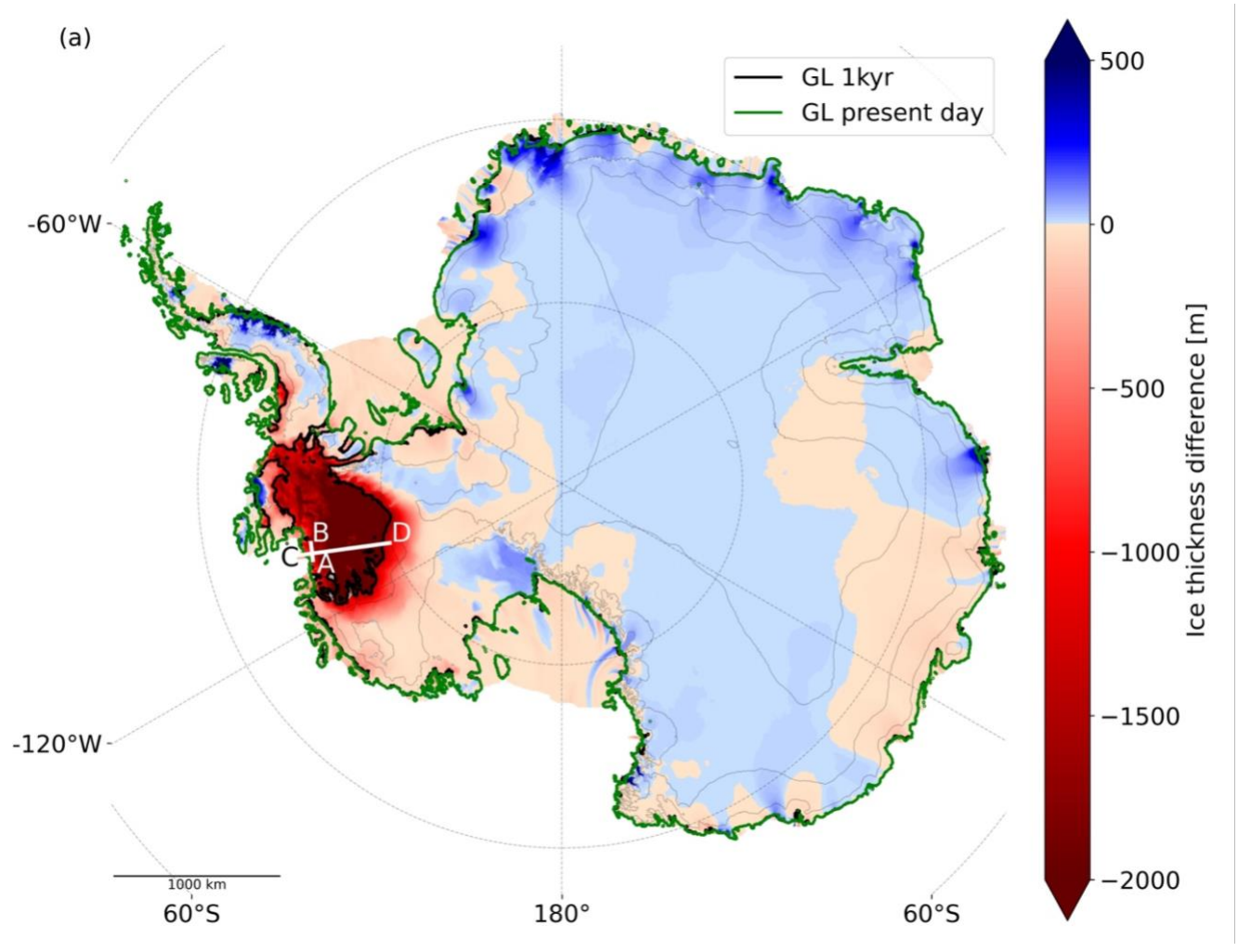

https://doi.org/10.5194/egusphere-2024-851
Preprint. Discussion started: 3 May 2024

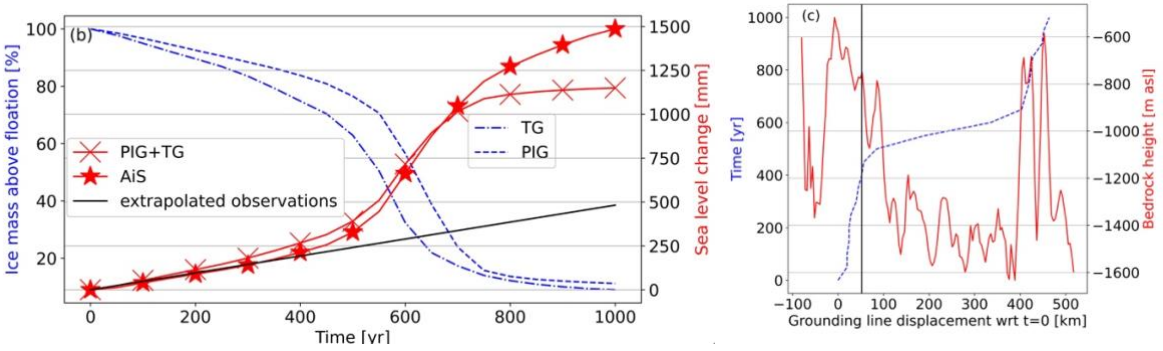

Figure 2. Future state of the Antarctic Ice Sheet. (a) Ice thickness change after a 1000-year continuation experiment initialized with present-day mass change rates. The original modeled GL resulting from the spin-up is shown in green, and the GL position at t = 1000 years is shown in black, only where it deviates from the spin-up GL. The thin grey lines show the modeled elevation with an interval of 1000 m at t=1000 years. (b) Ice mass above floatation for Thwaites Glacier (TG) and Pine Island Glacier (PIG) in blue, relative to the initial state shown in Fig. 1, and the corresponding sea level equivalent (calculated according to Eq 2 in Goelzer et al. (2020)) of TG, PIG (combined, crosses) and the AIS (stars) in red. Present-day observed mass loss is extrapolated in time and labeled as extrapolated observations in black. (c) GL displacement over time, and the bedrock profile along cross section *CD*. The last ridge before collapse is initiated, *AB*, is shown with a vertical black line. Once the GL passes this ridge, mass loss accelerates. A zoomed-in figure including the 2D bedrock profile is shown in Extended Data Fig. S7.

After 400 years, the mass loss accelerates as both PIG and TG collapse. The TG GL recedes faster than that of PIG (Fig. 2b). After 500 years, when the collapse is under way, ice velocities in the main channel of TG exceed 4000 m/yr, about twice the current modeled values (Fig. 3e). Thinning is greatest around the new GL, which is on a retrograde bed and therefore deeper than the current GL. Ocean thermal forcing in the ASE increases with depth since the melting point of ice decreases with increasing pressure (Jourdain et al., 2020); therefore newly ungrounded grid cells have a high basal melt rate and thin rapidly. After 750 years, TG and PIG have collapsed, and the basins contain almost no grounded ice, except on a few small ridges with bedrock above sea level. A large ice shelf has formed instead. At that time, the two basins have contributed about 1.2 meters to global sea level. Hence, the retreat of TG and PIG consists of two phases: a gradual linear decrease for the first few centuries, followed by an accelerated collapse, which continues until the basins are empty.

https://doi.org/10.5194/egusphere-2024-851
Preprint. Discussion started: 3 May 2024

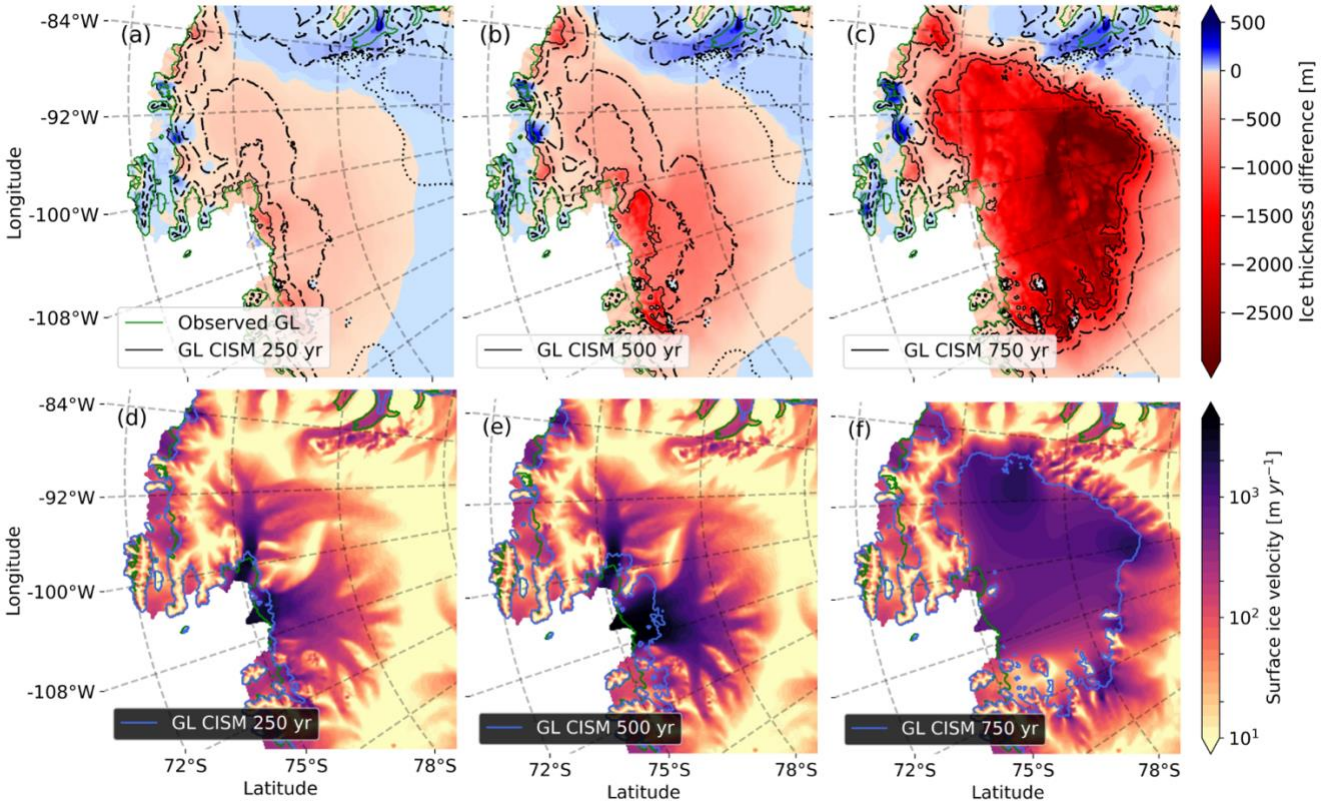

Figure 3. Development of the collapse at three times. (Top) Ice thickness difference with respect to the end of the initialization at t=250 yr (a), t=500 yr (b) and t=750 yr (c) after the start of the default continuation experiment. The present-day GL from observations is shown in green, and the modeled GL is shown in black. The ice surface elevation lines are contours of 500 (dashed), 1000 (dash-dotted) and 2000 (dotted) meters. (Bottom) Ice surface velocities at t=250 (d), t=500 (e) and t=750 (f) years, with the modeled GL shown in blue, and the observed GL in green.

During the whole continuation experiment, the collapse can be halted by turning off basal melting completely (Fig. S8). This is equivalent to decreasing ocean temperatures up to 4 K near the GL and on average 2–3 K elsewhere. To test whether the retreat is irreversible under realistic conditions, we ran experiments with ocean temperatures lowered at certain moments in the future. For example, the collapse can be stopped by cooling the ocean by 2 K relative to present-day values after 250 years. After 500 years, the collapse can be stopped only by ocean cooling of more than 2.5 K.

Hence, the accelerated collapse resembles the marine ice sheet instability (MISI) mechanism (Schoof, 2012, Schoof and Hewitt, 2013). However, the analytical solution of Schoof (2012) and Schoof and Hewitt (2013) does not account for an initial buttressing shelf and is valid only when there is no change in buttressing. Recently, two studies indicated that the current TG ice shelves provide little to no buttressing (Gudmundsson et al., 2019, Gudmundsson et al., 2023). During and after the modeled

https://doi.org/10.5194/egusphere-2024-851
Preprint. Discussion started: 3 May 2024

collapse, however, a large ice shelf forms, providing significant buttressing. As a result, ongoing basal melting is needed to overcome the increased buttressing and sustain the retreat. Stopping the basal melt would stop the collapse (see Fig. S8). Hence, we do not refer to the collapse as pure MISI following the analytical "Schoof" definition (Schoof, 2012), since the retreat would not proceed unabated if ocean thermal forcing were removed.

It is still debated whether the presence of warm CDW, about 3–4 degrees K above the melting point (Jacobs et al., 2011), under the PIG and TG shelves is a result of natural variability (Holland et al., 2019, Silvano et al., 2022) or forced by climate change. One model study (Holland et al., 2019) found that present-day WAIS basal melting is partly caused by internal variability and partly anthropogenically forced. In the former case, CDW might be (partly) absent in the future, lowering the melt rates. We therefore tested a range of values of ocean forcing and melt rates. When we first run 50 years into the future with the default initialization and then instantly halved the melt rates, the collapse is delayed but not halted. This suggests that if as much as half of the current basal melting is anthropogenically forced (e.g., from increased greenhouse gases and/or reduced stratospheric ozone), TG and PIG are still vulnerable to collapse.

5. Model choices and parameter value exploration

The results presented in Section 4 are based on the best estimate of the current system state, the preferred model parameterizations and their optimal parameter setting. To assess if the model results are robust within the observational and model uncertainties, we picked of each source of uncertainty, values that are on the edge of being realistic. The aim of these experiments is to find which process can prevent the projected collapse, hence might indicate that the default evolution of collapse is incorrect.

Figure 4 and Table 3 show the relative mass loss and resulting GMSL rise for this set of model choices and parameter values. Notably, the continuation of present-day climate forcing leads to TG and PIG collapse in all experiments. Once a collapse is initiated (i.e., when the mass loss accelerates), mass loss rates are similar, and all experiments show the same collapse duration (150 – 250 years, see Table 3). During the fast phase, the mass loss rate reaches about 3 mm GMSL/yr for almost every experiment. This is irrespective of the parameter setting, suggesting that the collapse rate is controlled by the bed topography and/or internal system dynamics rather than detailed physics or parameter choices.

The collapse timing is insensitive to the basal friction law (in line with (Barnes and Gudmundsson, 2022), model resolution (8 km or 4 km), and a 20% increase in the integrated SMB. Also, glacial isostatic adjustment (GIA), estimated using an Elastic Lithosphere Relaxing Asthenosphere (ELRA) model (Lambeck and Nakiboglu, 1980) with a relaxation time of 3000 yr, has little impact on glacier stability. GIA with a very short relaxation time of 100 yr delays the collapse by several centuries but does not prevent it. These findings are similar to the ones in Berdahl et al. (2023).

https://doi.org/10.5194/egusphere-2024-851
Preprint. Discussion started: 3 May 2024

The collapse timing is sensitive to model choices related to basal melting. A weaker/stronger dependence of the basal melt on the thermal forcing at the ice draft depth (Jourdain et al., 2020) delays/advances the start of the collapse (Berdahl et al. 2023). Taking a conservative approach by assuming no melt in a grid cell containing the GL (NMP) instead of partial melt (PMP) delays but does not prevent a collapse.

The UFEMISM simulations show a similar pattern of mass loss as the simulations conducted using CISM. Again, a linear phase of ice mass loss is modeled, and when approximately 30% of the original ice mass above floatation has disappeared, the accelerated collapse phase is initiated which lasts approximately 200 years when employing FCMP and 250 years when employing NMP. The similar behavior of the UFEMISM simulations suggests it is unlikely that the WAIS collapse modelled in CISM is a model-dependent feature, but the large difference in timing of the collapse highlights that the choice of ice sheet model is the largest source of uncertainty in this study with respect to the timing of the collapse.

In all simulations, there is first a nearly linear grounding line retreat with WAIS mass loss similar to the present day. This slow retreat phase is followed by accelerated retreat leading to Pine Island and Thwaites collapse. This behavior is in line with several earlier papers that did not include present-day mass change rates and therefore had to rely, for example, on ocean temperature (basal melt rate) perturbations (Joughin et al., 2014, Arthern and Williams, 2017, Golledge et al., 2021, Coulon et al., 2023). The ice loss rate during the collapse phase (~3 mm slr /yr), is similar to simulations done in those studies.

It would be interesting to study simultaneous changes in multiple parameters and physical choices. However, when combining two conservative model choices, e.g. NMP and low melt sensitivity to thermal forcing, the inversion procedure sometimes fails to reproduce the observed GL location. For this reason, and because most combinations require a separate, computationally expensive initialization, we did not consider combined effects of changing multiple parameters at once. To generate a single conservative end-member, we combined the two most conservative runs ("*No-melt parameterization at the GL*" and "*ELRA isostasy, relaxation time = 100 years*" in Table 1) into a "most conservative estimate." In this simulation, TG and PIG collapse after 2500 years (not shown in Fig. 4).

https://doi.org/10.5194/egusphere-2024-851
Preprint. Discussion started: 3 May 2024

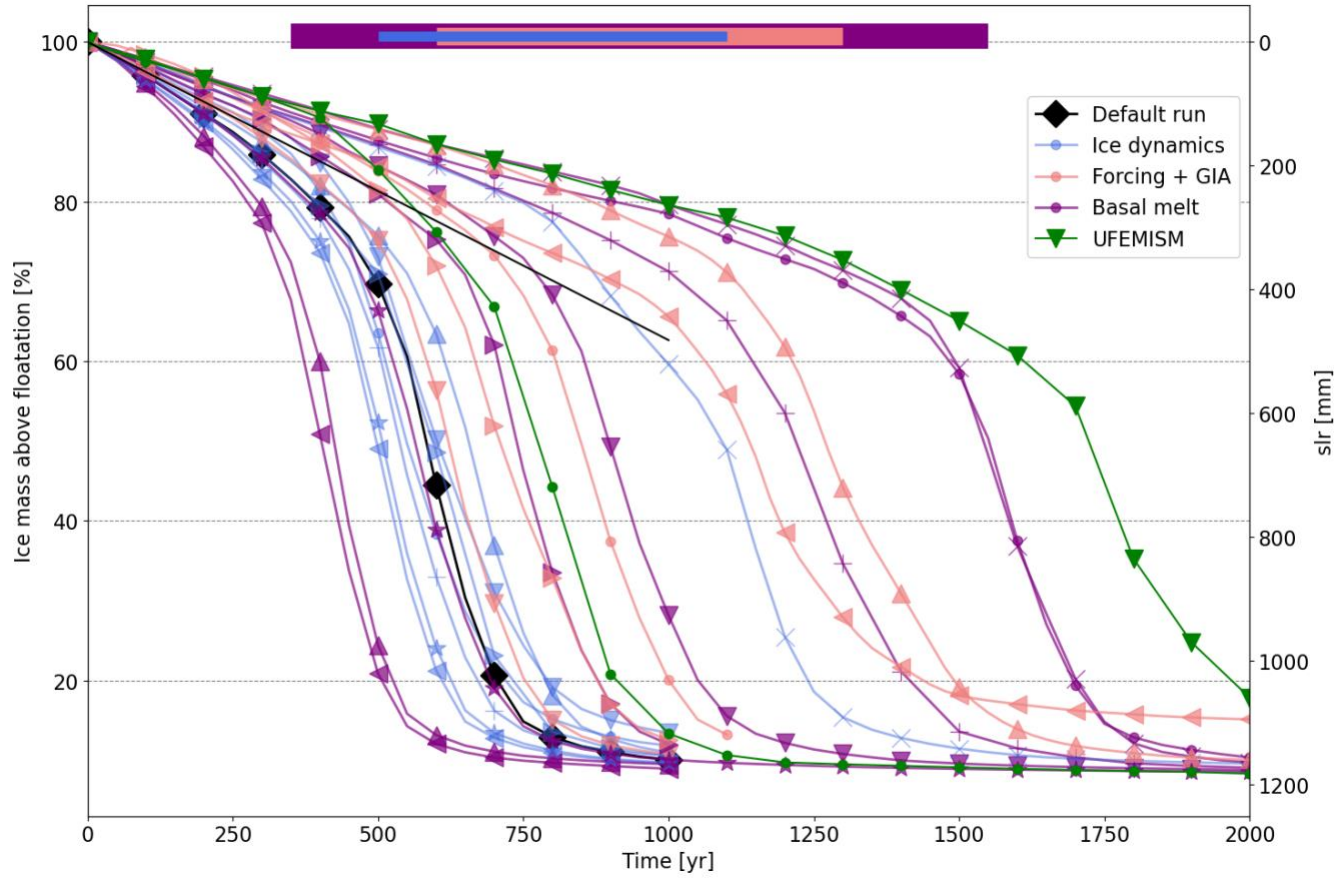

Figure 4. Sensitivity analysis. Ice mass above floatation (left y-axis) and resulting sea level rise (right axis) in the combined Thwaites and Pine Island Glacier basins for different experiments (22 in total). The mass change is calculated as the percentage difference relative to the initial value for the areas highlighted in Fig. 1a by orange polygons. The default run shown in Fig. 2 is plotted with black diamonds. The UFEMISM runs are shown in green, and the extrapolated observations as in Fig. 2b are shown in marker-free black. Most runs start with the observed mass change rates but deviate early in the run due to dynamic feedbacks. Some runs, e.g. "*SMB increases by 20% instantly"* start with different mass change rates. This explains the spreading trajectories in the first 100 years. The colored bars at the top indicate the range of times that the simulations reach 50% of their present-day ice volume, to highlight the uncertainty related to different categories. See Table 1 for a description of each run.

https://doi.org/10.5194/egusphere-2024-851
Preprint. Discussion started: 3 May 2024

Run description (full description in Extended Data Table 1)	**collapse initiated [yr]**	**collapse completed [yr]**	**Marker**
8km grid, partial melt parameterization (Leguy et al., 2021) *	300	500	
Highest basal melt versus depth sensitivity from ref. (Jourdain et al., 2020)	300	550	
Larger flow factor (softer ice) *	400	600	
No ocean connection ((Leguy et al., 2021) *	400	650	
With Schoof basal sliding parameterization, based on ref. (Asay-Davis et al., 2016)	450	650	
With a power-law basal sliding parameterization (Schoof 2007)*	450	700	
Thermal forcing capped at the maximum found at the GL	500	700	
Default continuation experiment	500	700	
ELRA isostasy, relaxation time = 3000 years	500	700	
With a Weertman power-law basal sliding parameterization	450	700	
SMB increases by 20% instantly	500	750	
Smaller flow factor (stiffer ice) *	550	800	
Mass change rates applied only on ice shelves*	600	900	
8-km grid, flotation-condition melt parameterization (Leguy et al., 2021)*	650	900	
Decrease basal melt rates after 50 years by 25%	700	950	
UFEMISM, partial melt parameterization*	700	950	
Flotation condition melt parameterization (Leguy et al., 2021)*	800	1050	
ELRA isostasy, relaxation time = 100 years	1100	1200	
Full ocean connection (Leguy et al., 2021) *	1100	1250	
Lowest basal melt versus thermal forcing sensitivity from ref. (Jourdain et al., 2020)	1200	1400	
Decrease basal melt rates after 50 years by 50%	1200	1350	
No-melt parameterization at the GL (Leguy et al., 2021) *	1500	1700	
8-km grid, no-melt parameterization (Leguy et al., 2021) *	1500	1700	
UFEMISM, floatation-condition melt parameterization	1600	1850	

https://doi.org/10.5194/egusphere-2024-851
Preprint. Discussion started: 3 May 2024

Table 3. Summary of the sensitivity experiments. Descriptions of the runs shown in Fig. 4. Except as noted otherwise, all settings and resolutions are the same as for the default initialization and continuation run. For some runs, denoted by an asterisk*, a new initialized state was needed. An extended description of each run can be found in Extended Data Table S1. The year of collapse initiation is defined as the year when the rate of basin-wide mass loss exceeds a 10% change in initial mass per 75 years (0.13%/year), which is equivalent to 1.72 mm GMSL/yr. The end of the collapse is defined as the first time the mass loss drops below this threshold again.

6. Conclusions and outlook

We have developed a new method to incorporate present-day mass change rates in an AIS model initialization. Given these observed rates, we show that for a wide range of (conservative) model choices, Thwaites Glacier and Pine Island Glacier will ultimately collapse, likely within 1000 years. These results are consistent with several previous studies (e.g., (Favier et al., 2014, Joughin et al., 2014), but carried out with an improved initialization scheme, a much wider range of model configurations, and without additional climate forcing. The timing of collapse onset is sensitive to model details and potential natural variability in ocean temperatures, but the length of the fast collapse phase, about 200 years, is not. This collapse is irreversible for the current climate and can probably be averted only by a large decrease in sub-shelf ocean temperatures. The collapse will likely begin sooner if Amundsen sub-shelf cavities were to warm further in the next few decades, as projected by a recent ocean modelling study (Naughten et al., 2023).

Since present-day ocean conditions and subsequently basal melt rates in ASE cavities do not seem to be able to coexist with the present-day geometry in steady state, it is likely that the cavities warmed during the past century when a different geometry was present. GCMs and high-resolution regional models could be used to simulate the coupled ice–ocean–atmosphere processes that might have triggered the recent warming. These models could also explore whether future anthropogenic action could cool these cavities enough to prevent collapse. Replication of our experiments with other ice sheet models could confirm our results and perhaps better constrain the timing of the collapse. We hypothesize that other models, like CISM and UFEMISM, will simulate collapse of TG and PIG on timescales of several centuries if the ocean forcing is sufficient to reproduce present-day thinning rates.

Data and code availability

Datasets used as input or calibration: bedrock profile and ice thickness from Morlighem et al. (2020), ice surface velocities from Rignot et al. (2019), ocean temperatures from Jourdain et al. (2020), surface mass balance from Van Wessem et al. (2018), geothermal heat flux from Martos et al. (2017), and mass changes rates from Smith et al. (2020) .

https://doi.org/10.5194/egusphere-2024-851
Preprint. Discussion started: 3 May 2024

The Community Ice Sheet Model 2.1.1 (CISM) and the Utrecht Finite Volume Ice-Sheet model UFEMISM v1.0 are both freely available on GitHub.

Author contributions

TvdA designed and executed the main experiments and the sensitivity analysis. WHL and GRL developed CISM and helped configure the model for the experiments. CJB and JAB performed the UFEMISM experiments and processed the data for the sensitivity analysis. RSWvdW and WJvdB provided guidance and feedback. TvdA prepared the manuscript, with contributions from all authors.

TvdA received funding from the NPP programme of the NWO. WHL and GRL were supported by the NSF National Center for Atmospheric Research, which is a major facility sponsored by the National Science Foundation (NSF) under Cooperative Agreement no. 1852977. Computing and data storage resources for CISM simulations, including the Cheyenne supercomputer (https://doi.org/10.5065/D6RX99HX), were provided by the Computational and Information Systems Laboratory (CISL) at NSF NCAR. GRL received additional support from NSF grant no. 2045075. CJB was supported by PROTECT. This project has received funding from the European Union's Horizon 2020 research and innovation program under grant agreement no. 869304. JB received funding from NWO grant 515.

The authors declare no competing interests.

References

Adusumilli, S., H. A. Fricker, B. Medley, L. Padman and M. R. Siegfried (2020). "Interannual variations in meltwater input to the Southern Ocean from Antarctic ice shelves." Nature geoscience **13**(9): 616-620

Amaral, T., T. C. Bartholomaus and E. M. Enderlin (2020). "Evaluation of iceberg calving models against observations from Greenland outlet glaciers." Journal of Geophysical Research: Earth Surface **125**(6): e2019JF005444

Arthern, R. J. and C. R. Williams (2017). "The sensitivity of West Antarctica to the submarine melting feedback." Geophysical Research Letters **44**(5): 2352-2359

Asay-Davis, X. S., S. L. Cornford, G. Durand, B. K. Galton-Fenzi, R. M. Gladstone, G. H. Gudmundsson, T. Hattermann, D. M. Holland, D. Holland and P. R. Holland (2016). "Experimental design for three interrelated marine ice sheet and ocean model intercomparison projects: MISMIP v. 3 (MISMIP+), ISOMIP v. 2 (ISOMIP+) and MISOMIP v. 1 (MISOMIP1)." Geoscientific Model Development **9**(7): 2471-2497

Aschwanden, A., T. C. Bartholomaus, D. J. Brinkerhoff and M. Truffer (2021). "Brief communication: A roadmap towards credible projections of ice sheet contribution to sea level." The Cryosphere **15**(12): 5705-5715

Barnes, J. M. and G. H. Gudmundsson (2022). "The predictive power of ice sheet models and the regional sensitivity of ice loss to basal sliding parameterisations: a case study of Pine Island and Thwaites glaciers, West Antarctica." The Cryosphere **16**(10): 4291-4304

Berdahl, M., G. Leguy, W. H. Lipscomb, N. M. Urban and M. J. Hoffman (2023). "Exploring ice sheet model sensitivity to ocean thermal forcing and basal sliding using the Community Ice Sheet Model (CISM)." The Cryosphere **17**(4): 1513-1543

Berends, C. J., H. Goelzer, T. J. Reerink, L. B. Stap and R. S. Van De Wal (2022). "Benchmarking the vertically integrated ice-sheet model IMAU-ICE (version 2.0)." Geoscientific Model Development **15**(14): 5667-5688

Berends, C. J., H. Goelzer and R. S. Van De Wal (2021). "The Utrecht finite volume ice-sheet model: UFEMISM (version 1.0)." Geoscientific Model Development **14**(5): 2443-2470

https://doi.org/10.5194/egusphere-2024-851
Preprint. Discussion started: 3 May 2024

Bernales, J., I. Rogozhina, R. Greve and M. Thomas (2017). "Comparison of hybrid schemes for the combination of shallow approximations in numerical simulations of the Antarctic Ice Sheet." The Cryosphere **11**(1): 247-265

Bernales, J., I. Rogozhina and M. Thomas (2017). "Melting and freezing under Antarctic ice shelves from a combination of ice-sheet modelling and observations." Journal of Glaciology **63**(240): 731-744

Bradley, A. and R. Arthern (2021). WAVI. jl: A Fast, Flexible, and Friendly Modular Ice Sheet Model, Written in Julia. AGU Fall Meeting Abstracts.

Bueler, E. and J. Brown (2009). "Shallow shelf approximation as a "sliding law" in a thermomechanically coupled ice sheet model." Journal of Geophysical Research: Earth Surface **114**(F3)

Cornford, S. L., D. Martin, A. Payne, E. Ng, A. Le Brocq, R. M. Gladstone, T. L. Edwards, S. R. Shannon, C. Agosta and M. R. van den Broeke (2015). "Century-scale simulations of the response of the West Antarctic Ice Sheet to a warming climate." The Cryosphere **9**(4): 1579-1600

Coulon, V., A. K. Klose, C. Kittel, R. Winkelmann and F. Pattyn (2023). Disentangling the drivers of future Antarctic ice loss with a historically-calibrated ice-sheet model, EGUsphere [preprint].

Danabasoglu, G., J. F. Lamarque, J. Bacmeister, D. Bailey, A. DuVivier, J. Edwards, L. Emmons, J. Fasullo, R. Garcia and A. Gettelman (2020). "The community earth system model version 2 (CESM2)." Journal of Advances in Modeling Earth Systems **12**(2): e2019MS001916

Dow, C. F. (2019). How well does the equal-pressure hydraulic potential approach work for estimating subglacial hydrological networks? AGU Fall Meeting Abstracts.

Favier, L., G. Durand, S. L. Cornford, G. H. Gudmundsson, O. Gagliardini, F. Gillet-Chaulet, T. Zwinger, A. Payne and A. M. Le Brocq (2014). "Retreat of Pine Island Glacier controlled by marine ice-sheet instability." Nature Climate Change **4**(2): 117-121

Feldmann, J. and A. Levermann (2015). "Collapse of the West Antarctic Ice Sheet after local destabilization of the Amundsen Basin." Proceedings of the national academy of sciences **112**(46): 14191-14196

Flexas, M. M., A. F. Thompson, M. P. Schodlok, H. Zhang and K. Speer (2022). "Antarctic Peninsula warming triggers enhanced basal melt rates throughout West Antarctica." Science advances **8**(31): eabj9134

Fox-Kemper, B., C. X. H.T. Hewitt, G. Aðalgeirsdóttir, S. S. Drijfhout, T. L. Edwards, N. R. Golledge, M. Hemer, R. E. Kopp, G. Krinner, A. Mix, D. Notz, S. Nowicki, I. S. Nurhati, L. Ruiz, J.-B. Sallée, A. B. A. Slangen and Y. Yu. (2021). "Ocean, Cryosphere and Sea Level Change. In Climate Change 2021: The Physical Science Basis. Contribution of Working Group I to the Sixth Assessment Report of the Intergovernmental Panel on Climate Change " Cambridge University Press, Cambridge, United Kingdom and New York, NY, USA: 1211-1362

Garbe, J., T. Albrecht, A. Levermann, J. F. Donges and R. Winkelmann (2020). "The hysteresis of the Antarctic ice sheet." Nature **585**(7826): 538-544

Goelzer, H., V. Coulon, F. Pattyn, B. De Boer and R. Van De Wal (2020). "Brief communication: On calculating the sea-level contribution in marine ice-sheet models." The Cryosphere **14**(3): 833-840

Goldberg, D. N. (2011). "A variationally derived, depth-integrated approximation to a higher-order glaciological flow model." Journal of Glaciology **57**(201): 157-170

Golledge, N. R., P. U. Clark, F. He, A. Dutton, C. Turney, C. Fogwill, T. Naish, R. H. Levy, R. M. McKay and D. P. Lowry (2021). "Retreat of the Antarctic Ice Sheet during the Last Interglaciation and implications for future change." Geophysical Research Letters **48**(17): e2021GL094513

Greene, C. A., A. S. Gardner, N.-J. Schlegel and A. D. Fraser (2022). "Antarctic calving loss rivals ice-shelf thinning." Nature **609**(7929): 948-953

Greve, R. and H. Blatter (2016). "Comparison of thermodynamics solvers in the polythermal ice sheet model SICOPOLIS." Polar Science **10**(1): 11-23

Gudmundsson, G., J. Krug, G. Durand, L. Favier and O. Gagliardini (2012). "The stability of grounding lines on retrograde slopes." The Cryosphere **6**(6): 1497-1505

Gudmundsson, G. H., J. M. Barnes, D. Goldberg and M. Morlighem (2023). "Limited impact of Thwaites Ice Shelf on future ice loss from Antarctica." Geophysical Research Letters **50**(11): e2023GL102880

Gudmundsson, G. H., F. S. Paolo, S. Adusumilli and H. A. Fricker (2019). "Instantaneous Antarctic ice sheet mass loss driven by thinning ice shelves." Geophysical Research Letters **46**(23): 13903-13909

https://doi.org/10.5194/egusphere-2024-851
Preprint. Discussion started: 3 May 2024

Hellmer, H. H. (2004). "Impact of Antarctic ice shelf basal melting on sea ice and deep ocean properties." Geophysical Research Letters **31**(10)

Hoffman, M. J., M. Perego, S. F. Price, W. H. Lipscomb, T. Zhang, D. Jacobsen, I. Tezaur, A. G. Salinger, R. Tuminaro and L. Bertagna (2018). "MPAS-Albany Land Ice (MALI): a variable-resolution ice sheet model for Earth system modeling using Voronoi grids." Geoscientific Model Development **11**(9): 3747-3780

Holland, P. R., T. J. Bracegirdle, P. Dutrieux, A. Jenkins and E. J. Steig (2019). "West Antarctic ice loss influenced by internal climate variability and anthropogenic forcing." Nature Geoscience **12**(9): 718-724

Jacobs, S., A. Jenkins, C. Giulivi and P. Dutrieux (2011). "Stronger sub-ice shelf ocean circulation undermining the Pine Island Glacier." Nature Geoscience **4**: 519-523

Jacobs, S. S., A. Jenkins, C. F. Giulivi and P. Dutrieux (2011). "Stronger ocean circulation and increased melting under Pine Island Glacier ice shelf." Nature Geoscience **4**(8): 519-523

Jenkins, A., P. Dutrieux, S. Jacobs, E. J. Steig, G. H. Gudmundsson, J. Smith and K. J. Heywood (2016). "Decadal ocean forcing and Antarctic ice sheet response: Lessons from the Amundsen Sea." Oceanography **29**(4): 106-117

Joughin, I., B. E. Smith and B. Medley (2014). "Marine ice sheet collapse potentially under way for the Thwaites Glacier Basin, West Antarctica." Science **344**(6185): 735-738

Joughin, I., B. E. Smith and C. G. Schoof (2019). "Regularized Coulomb friction laws for ice sheet sliding: Application to Pine Island Glacier, Antarctica." Geophysical research letters **46**(9): 4764-4771

Jourdain, N. C., X. Asay-Davis, T. Hattermann, F. Straneo, H. Seroussi, C. M. Little and S. Nowicki (2020). "A protocol for calculating basal melt rates in the ISMIP6 Antarctic ice sheet projections." The Cryosphere **14**: 3111-3134

Kazmierczak, E., T. Gregov, V. Coulon and F. Pattyn (2024). "A fast and unified subglacial hydrological model applied to Thwaites Glacier, Antarctica." EGUsphere **2024**: 1-36

Lambeck, K. and S. Nakiboglu (1980). "Seamount loading and stress in the ocean lithosphere." Journal of Geophysical Research: Solid Earth **85**(B11): 6403-6418

Larour, E., H. Seroussi, M. Morlighem and E. Rignot (2012). "Continental scale, high order, high spatial resolution, ice sheet modeling using the Ice Sheet System Model (ISSM)." Journal of Geophysical Research: Earth Surface **117**(F1)

Leguy, G., X. Asay-Davis and W. Lipscomb (2014). "Parameterization of basal friction near grounding lines in a one-dimensional ice sheet model." The Cryosphere **8**(4): 1239-1259

Leguy, G. R., W. H. Lipscomb and X. S. Asay-Davis (2021). "Marine ice sheet experiments with the Community Ice Sheet Model." The Cryosphere **15**(7): 3229-3253

Lhermitte, S., S. Sun, C. Shuman, B. Wouters, F. Pattyn, J. Wuite, E. Berthier and T. Nagler (2020). "Damage accelerates ice shelf instability and mass loss in Amundsen Sea Embayment." Proceedings of the National Academy of Sciences **117**(40): 24735-24741

Lipscomb, W. H., G. R. Leguy, N. C. Jourdain, X. Asay-Davis, H. Seroussi and S. Nowicki (2021). "ISMIP6-based projections of ocean-forced Antarctic Ice Sheet evolution using the Community Ice Sheet Model." The Cryosphere **15**(2): 633-661

Lipscomb, W. H., S. F. Price, M. J. Hoffman, G. R. Leguy, A. R. Bennett, S. L. Bradley, K. J. Evans, J. G. Fyke, J. H. Kennedy and M. Perego (2019). "Description and evaluation of the community ice sheet model (CISM) v2. 1." Geoscientific Model Development **12**(1): 387-424

Martos, Y. M., M. Catalán, T. A. Jordan, A. Golynsky, D. Golynsky, G. Eagles and D. G. Vaughan (2017). "Heat flux distribution of Antarctica unveiled." Geophysical Research Letters **44**(22): 11,417-411,426

Milillo, P., E. Rignot, P. Rizzoli, B. Scheuchl, J. Mouginot, J. Bueso-Bello and P. Prats-Iraola (2019). "Heterogeneous retreat and ice melt of Thwaites Glacier, West Antarctica." Science advances **5**(1): eaau3433

Morlighem, M., E. Rignot, T. Binder, D. Blankenship, R. Drews, G. Eagles, O. Eisen, F. Ferraccioli, R. Forsberg and P. Fretwell (2020). "Deep glacial troughs and stabilizing ridges unveiled beneath the margins of the Antarctic ice sheet." Nature Geoscience **13**(2): 132-137

Naughten, K. A., P. R. Holland and J. De Rydt (2023). "Unavoidable future increase in West Antarctic ice-shelf melting over the twenty-first century." Nature Climate Change

Naughten, K. A., P. R. Holland, P. Dutrieux, S. Kimura, D. T. Bett and A. Jenkins (2022). "Simulated twentieth-century ocean warming in the Amundsen Sea, West Antarctica." Geophysical Research Letters **49**(5): e2021GL094566

Pattyn, F., C. Ritz, E. Hanna, X. Asay-Davis, R. DeConto, G. Durand, L. Favier, X. Fettweis, H. Goelzer and N. R. Golledge (2018). "The Greenland and Antarctic ice sheets under 1.5 C global warming." Nature Climate Change **8**(12): 1053-1061

https://doi.org/10.5194/egusphere-2024-851
Preprint. Discussion started: 3 May 2024

Payne, A. J., S. Nowicki, A. Abe-Ouchi, C. Agosta, P. Alexander, T. Albrecht, X. Asay-Davis, A. Aschwanden, A. Barthel and T. J. Bracegirdle (2021). "Future sea level change under coupled model intercomparison project phase 5 and phase 6 scenarios from the Greenland and Antarctic ice sheets." Geophysical Research Letters **48**(16): e2020GL091741

Pollard, D. and R. DeConto (2012). "Description of a hybrid ice sheet-shelf model, and application to Antarctica." Geoscientific Model Development **5**(5): 1273-1295

Quiquet, A., C. Dumas, C. Ritz, V. Peyaud and D. M. Roche (2018). "The GRISLI ice sheet model (version 2.0): calibration and validation for multi-millennial changes of the Antarctic ice sheet." Geoscientific Model Development **11**(12): 5003-5025

Reese, R., J. Garbe, E. A. Hill, B. Urruty, K. A. Naughten, O. Gagliardini, G. Durand, F. Gillet-Chaulet, G. H. Gudmundsson and D. Chandler (2023). "The stability of present-day Antarctic grounding lines–Part 2: Onset of irreversible retreat of Amundsen Sea glaciers under current climate on centennial timescales cannot be excluded." The Cryosphere **17**(9): 3761-3783

Rémy, F. and B. Legresy (2004). "Subglacial hydrological networks in Antarctica and their impact on ice flow." Annals of Glaciology **39**: 67-72

Rignot, E., S. Jacobs, J. Mouginot and B. Scheuchl (2013). "Ice-shelf melting around Antarctica." Science **341**(6143): 266-270

Rignot, E., J. Mouginot, M. Morlighem, H. Seroussi and B. Scheuchl (2014). "Widespread, rapid grounding line retreat of Pine Island, Thwaites, Smith, and Kohler glaciers, West Antarctica, from 1992 to 2011." Geophysical Research Letters **41**(10): 3502-3509

Rignot, E., J. Mouginot, B. Scheuchl, M. Van Den Broeke, M. J. Van Wessem and M. Morlighem (2019). "Four decades of Antarctic Ice Sheet mass balance from 1979–2017." Proceedings of the National Academy of Sciences **116**(4): 1095-1103

Robinson, A., D. Goldberg and W. H. Lipscomb (2022). "A comparison of the stability and performance of depth-integrated ice-dynamics solvers." The Cryosphere **16**(2): 689-709

Rosier, S. H., R. Reese, J. F. Donges, J. De Rydt, G. H. Gudmundsson and R. Winkelmann (2021). "The tipping points and early warning indicators for Pine Island Glacier, West Antarctica." The Cryosphere **15**(3): 1501-1516

Schoof, C. (2012). "Marine ice sheet stability." Journal of Fluid Mechanics **698**: 62-72

Schoof, C. and I. Hewitt (2013). "Ice-sheet dynamics." Annual Review of Fluid Mechanics **45**: 217-239

Seroussi, H., S. Nowicki, A. J. Payne, H. Goelzer, W. H. Lipscomb, A. Abe-Ouchi, C. Agosta, T. Albrecht, X. Asay-Davis and A. Barthel (2020). "ISMIP6 Antarctica: a multi-model ensemble of the Antarctic ice sheet evolution over the 21st century." The Cryosphere **14**(9): 3033-3070

Seroussi, H., S. Nowicki, E. Simon, A. Abe-Ouchi, T. Albrecht, J. Brondex, S. Cornford, C. Dumas, F. Gillet-Chaulet and H. Goelzer (2019). "initMIP-Antarctica: an ice sheet model initialization experiment of ISMIP6." The Cryosphere **13**(5): 1441-1471

Silvano, A., P. R. Holland, K. A. Naughten, O. Dragomir, P. Dutrieux, A. Jenkins, Y. Si, A. L. Stewart, B. Peña Molino and G. W. Janzing (2022). "Baroclinic Ocean Response to Climate Forcing Regulates Decadal Variability of Ice-Shelf Melting in the Amundsen Sea." Geophysical Research Letters **49**(24): e2022GL100646

Smith, B., H. A. Fricker, A. S. Gardner, B. Medley, J. Nilsson, F. S. Paolo, N. Holschuh, S. Adusumilli, K. Brunt and B. Csatho (2020). "Pervasive ice sheet mass loss reflects competing ocean and atmosphere processes." Science **368**(6496): 1239-1242

Sun, S., F. Pattyn, E. G. Simon, T. Albrecht, S. Cornford, R. Calov, C. Dumas, F. Gillet-Chaulet, H. Goelzer and N. R. Golledge (2020). "Antarctic ice sheet response to sudden and sustained ice-shelf collapse (ABUMIP)." Journal of Glaciology **66**(260): 891-904

Swart, N. C., T. Martin, R. Beadling, J.-J. Chen, C. Danek, M. H. England, R. Farneti, S. M. Griffies, T. Hattermann and J. Hauck (2023). "The Southern Ocean Freshwater Input from Antarctica (SOFIA) Initiative: scientific objectives and experimental design." Geoscientific Model Development **16**(24): 7289-7309

Thoma, M., A. Jenkins, D. Holland and S. Jacobs (2008). "Modelling circumpolar deep water intrusions on the Amundsen Sea continental shelf, Antarctica." Geophysical Research Letters **35**(18)

van de Wal, R. S., R. J. Nicholls, D. Behar, K. McInnes, D. Stammer, J. A. Lowe, J. A. Church, R. DeConto, X. Fettweis and H. Goelzer (2022). "A High-End Estimate of Sea Level Rise for Practitioners." Earth's future **10**(11): e2022EF002751

van der Wel, N., P. Christoffersen and M. Bougamont (2013). "The influence of subglacial hydrology on the flow of Kamb Ice Stream, West Antarctica." Journal of Geophysical Research: Earth Surface **118**(1): 97-110

https://doi.org/10.5194/egusphere-2024-851
Preprint. Discussion started: 3 May 2024

Van Wessem, J. M., W. J. Van De Berg, B. P. Noël, E. Van Meijgaard, C. Amory, G. Birnbaum, C. L. Jakobs, K. Krüger, J. T. Lenaerts and S. Lhermitte (2018). "Modelling the climate and surface mass balance of polar ice sheets using RACMO2–Part 2: Antarctica (1979–2016)." The Cryosphere **12**(4): 1479-1498

Wilner, J. A., M. Morlighem and G. Cheng (2023). "Evaluation of four calving laws for Antarctic ice shelves." The Cryosphere Discussions **2023**: 1-19

Winkelmann, R., M. A. Martin, M. Haseloff, T. Albrecht, E. Bueler, C. Khroulev and A. Levermann (2011). "The Potsdam parallel ice sheet model (PISM-PIK)–Part 1: Model description." The Cryosphere **5**(3): 715-726

Yu, H., E. Rignot, H. Seroussi, M. Morlighem and Y. Choi (2019). "Impact of iceberg calving on the retreat of Thwaites Glacier, West Antarctica over the next century with different calving laws and ocean thermal forcing." Geophysical Research Letters **46**(24): 14539-14547

Zoet, L. K. and N. R. Iverson (2020). "A slip law for glaciers on deformable beds." Science **368**(6486): 76-78